Volume I, Executive Summary

CR-184071

GE Astro Space

Final Study Report
Phase I

Contract No. NAS8-37589
26 March 1990

Definition and Preliminary Design of the LAWS Laser Atmospheric Wind Sounder

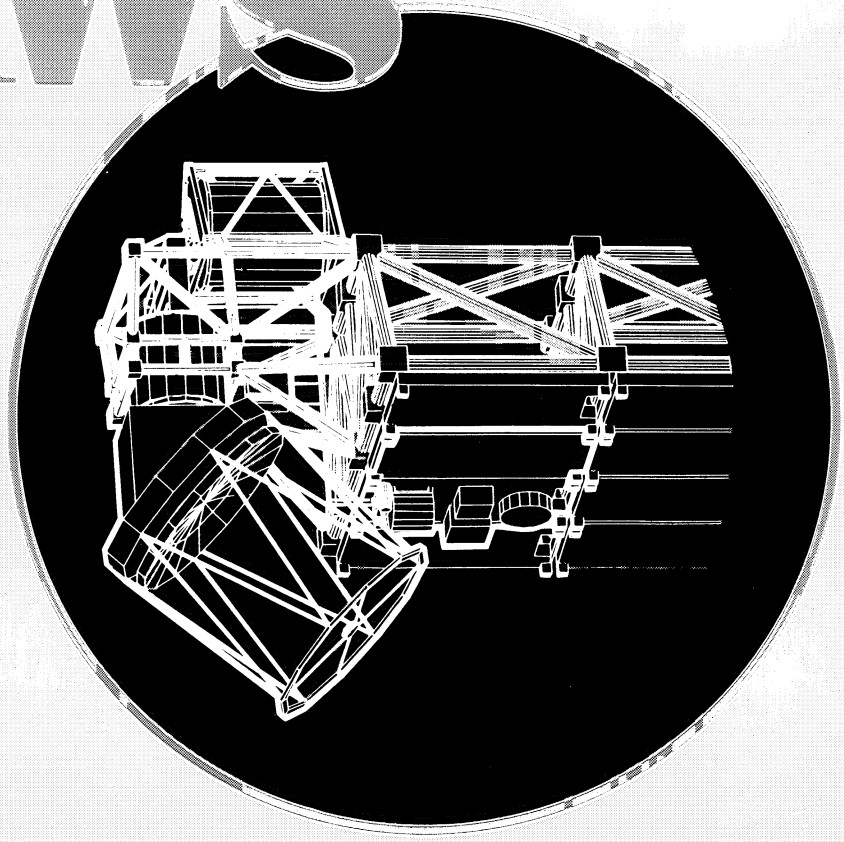

Marshall Space Flight Center

GE Astro Space
Hughes Danbury
Spectra Technology

GE Astro Space Division
PO Box 8555
Philadelphia, PA 19101

Definition and Preliminary Design of the

LAWS

Laser Atmospheric
Wind Sounder

PHASE I
FINAL REPORT VOLUME I

EXECUTIVE SUMMARY

Date: 3/26/90
(Final Submission: 5/15/90)

Contract Number: NAS8-37589

GE Astro Space
Hughes Danbury
Spectra Technology

TABLE OF CONTENTS

LIST OF FIGURES

LIST OF TABLES

EXECUTIVE SUMMARY

1.0. INTRODUCTION

The Laser Atmospheric Wind Sounder (LAWS) Study (Phase I) was conducted by GE Astro-Space Division, with the support of Hughes Danbury Optical Systems (formerly Perkin-Elmer) for the optical subsystem and Spectra Technology for the laser subsystem. Lassen Research and Simpson Weather Associates also provided support in the areas of receiver signal processor and mission analysis, respectively. The contract was managed by the NASA Marshall Space Flight Center and performed over a 12-month period from March 27, 1989 to March 26, 1990.

LAWS, which is a facility instrument of the Earth Observing System (EOS), is the culmination of over 20 years of effort in the field of laser Doppler wind sensing and will be the first instrument to fly in space capable of providing global-scale tropospheric wind profiles at high spatial resolutions. Global-scale wind profiles are necessary for:

- More accurate diagnostics of large-scale circulation and climate dynamics;
- Improved numerical weather prediction;
- Improved understanding of mesoscale systems;
- Improved understanding of global biogeochemical and hydrologic cycles.

The objective of phase I of the LAWS study was to evaluate competing concepts and develop a baseline configuration for the LAWS instrument. The first phase of the study consisted of identifying realistic concepts for LAWS and analyzing them in sufficient detail to be able to choose the most promising one for the LAWS application. System configurations were then developed for the chosen concept. The concept and subsequent configuration were to be compatible with two prospective platforms-- the Japanese Polar Orbiting Platform (JPOP) and the Space Station Freedom (as an attached payload).

After an objective and comprehensive concept selection process, we chose a heterodyne detection Doppler lidar using a CO_2 laser transmitter operating at 9.1 μm over a 2.1 μm system with a solid state laser. The choice of CO_2 over solid state reflects the advanced state of development of CO_2 lasers and the eased subsystem requirements associated with the longer wavelength.

The CO_2 lidar concept was then analyzed in detail to arrive at a configuration for the instrument and its major subsystems. Our approach throughout the configuration design was to take a system perspective and trade requirements between subsystems to reduce technical risk and system cost. Wherever possible, we worked to arrive at configurations which made maximum use of existing, proven technology or were

relatively straightforward extensions of existing technology. At the conclusion of Phase I, we arrived at a configuration for LAWS which meets the performance requirements, yet which is less complex than previous designs of space-based wind sensors (e.g. Windsat), employs lightweight technologies to meet its weight goal (<800 kg) and is sufficiently flexible to offer various operational scenarios with power requirements from about 2 kW to 3 kW. Highlights of the design are:

- A unitary construction, compact, lightweight, efficient laser with substantial heritage including the proven NOAA Windvan design. The laser uses the oxygen-18 isotope of CO_2 to increase atmospheric transmission; a combination of funded and in-house measurement programs have shown that the use of this gas is a straightforward extension of techniques developed with the normal oxygen-16 isotope. The laser operates asynchronously at up to 20 Hz maximum repetition rate and therefore offers a variety of measurement scenarios.
- A new optical subsystem design which is simpler than the previous Windsat design and overcomes known Windsat design deficiencies. The optical subsystem fully supports asynchronous operation by eliminating the mechanisms for lag angle compensation and transmit-receive switching.
- A receiver subsystem which uses a circularly symmetric array detector to increase the total received signal, enable an end-to-end closed loop alignment and control system by measuring the phase distribution of the returned signal, and provide a degree of redundancy. The receiver design benefits from significant in-house development of mercury-cadmium-telluride (MCT) detectors and arrays aimed at increasing the quantum efficiencies at the high bandwidths necessary for LAWS.
- Extensive use of existing technology for the support subsystems including: a graphite-epoxy truss support structure based on the GE technology developed for UARS and the Space Station Polar Platforms Work Package 3 (WP-3); a thermal subsystem based on heat pipe and capillary-pumped loop technology employed in WP-3; a momentum compensation approach from an in-house communications satellite program (GSTAR); and system controller computer technology from Space Station.

Further details of the Phase I concept selection are given below in section 2.0. Design and specifications for the system and subsystem configurations follow in section 3.0, and LAWS system performance is outlined in section 4.0.

2.0 CONCEPT SELECTION

The top-level mission requirements which were used to discriminate between concepts for LAWS were:

- Horizontal wind profile resolution of 100 km x 100 km;
- Vertical Resolution of 1 km throughout the troposphere;
- Horizontal wind vector accuracy of ± 1 m/s in the lower troposphere and ± 5 m/s in the upper troposphere;
- Operational lifetime of 10^9 shots.

There are many ways of making wind measurements in the atmosphere using lasers which can satisfy some or all of the above requirements. To choose between them we needed an objective methodology which was capable of rejecting, early in the selection process, those concepts which were unrealistic in light of the requirements, yet which was fully capable of analyzing in detail those concepts which appeared feasible. To accomplish this we used a two part process. First, we structured the concepts in the form of a hierarchical decision tree which allowed us to quickly eliminate whole classes of unrealistic concepts. The decision tree is shown in Figure 1, where the shaded circles indicate the route taken through the tree and the open circles end in dialogue boxes which give a brief synopsis of the reasons for terminating that particular branch of the tree. After progressing through the decision tree we concluded there were two promising concepts for LAWS which required a more in-depth analysis. The two concepts both used heterodyne detection, but at different wavelengths, one being based on a Tm:Ho:YAG solid-state laser at 2.1 μm and the other a $^{12}C^{18}O_2$ gas laser operating at 9.1 μm.

To conduct the more detailed analysis we developed an evaluation and selection criteria plan. The plan consisted of a set of criteria against which to evaluate those concepts which made it through the decision tree. Concepts were broken down into component subsystems and scored against those criteria, which were weighted to reflect their relative importance. Weighted scores were then added for each concept. The scores for the 2.1 μm and 9.1 μm concepts are shown in Figure 2.

The scoring reflects both the state of development of lasers, optical subsystems and receivers for operation at 2.1 μm, as well as issues associated with the shorter wavelength. These include: the difficulty and cost of fabricating large diffraction limited optical telescopes, the increased pointing requirements because of the 4.5x smaller FOV, the 4.5x larger Doppler bandwidth (~8 GHz), the 4.5x larger measurement bandwidth (~200 MHz) which leads to a large increase in the data rate for the shorter wavelength, and atmospheric turbulence. The overall scores show that the 9.1 μm concept is the

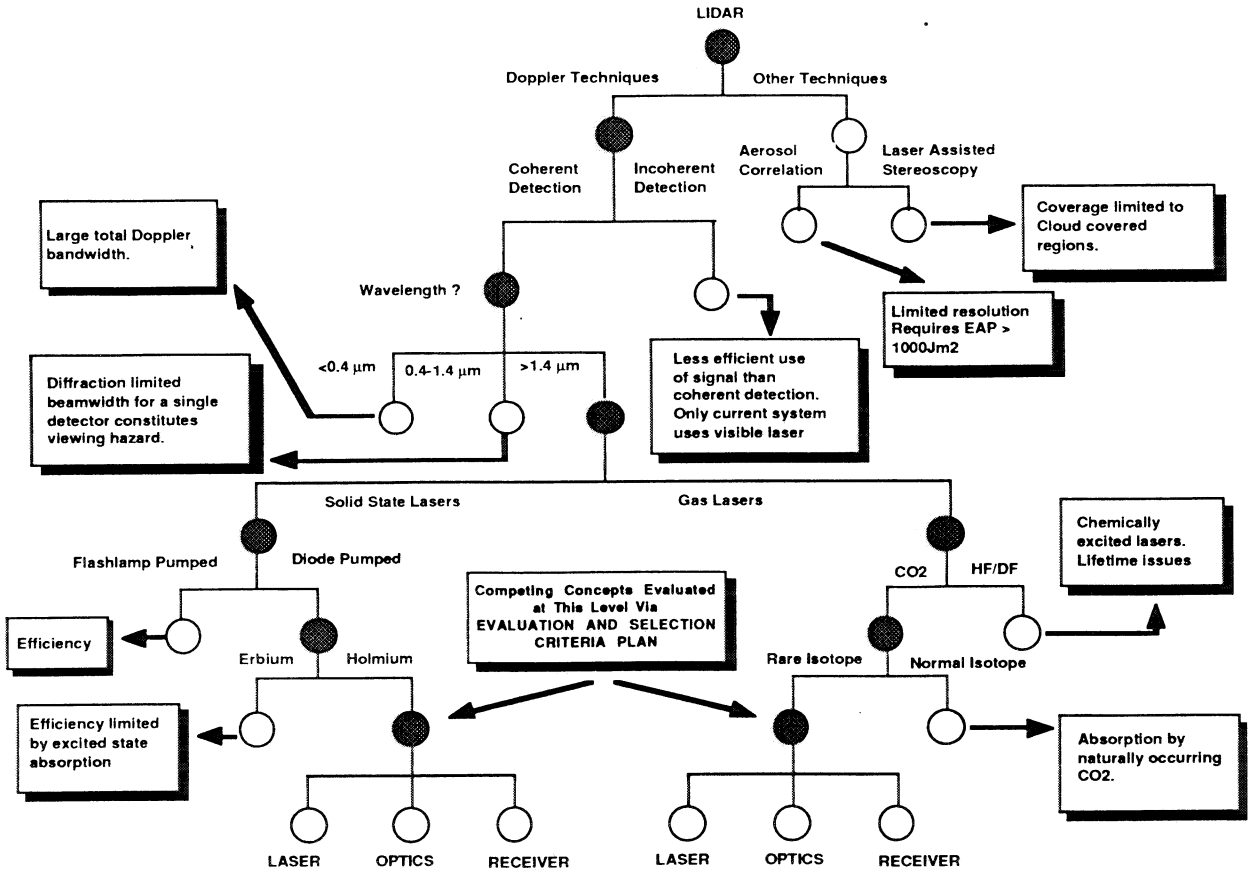

Figure 1. Decision Tree Illustrating the Route Taken for Concept Selection

clear choice for LAWS with the primary consideration being the mature state of the art for CO_2 lasers versus the immature and unproven technology for large scale, eye-safe wavelength, solid state lasers.

We therefore selected as the concept for the LAWS instrument a 9.1 μm $^{12}C^{18}O_2$ laser operating in the heterodyne mode with a Mercury-Cadmium-Telluride (MCT) detector in the focal plane of a conically-scanned telescope.

SUBSYSTEMS/COMPONENTS	SELECTION CRITERIA												
	PERFORMANCE	TECHNOLOGY	DESIGN SIMPLICITY	RELIABILITY	ACCOMMODATIONS	SERVICEABILITY	SYSTEM OPERATIONS	VERIFICATION	RISK	SURVIVABILITY	COST	SAFETY	TOTAL SCORE
WEIGHTING FACTOR	4	4	3	3	3	2	2	3	5	2	4	N/A	
2.1 μm CONCEPT													
LASER SUBSYSTEM	2/8	2/8	2/6	2/6	4/12	3/6	4/8	2/6	1/5	2/4	2/8	1	77
OPTICAL SUBSYSTEM	2/8	3/12	3/9	3/12	4/12	1/2	4/8	3/9	1/5	5/10	2/8	1	95
RECEIVER SUBSYSTEM	4/16	3/12	4/12	3/9	5/15	5/10	5/10	3/9	2/10	3/6	3/12	1	121
9.1 μm CONCEPT													
LASER SUBSYSTEM	4/16	5/20	4/12	3/9	4/12	3/6	4/8	3/9	3/15	4/8	3/12	1	127
OPTICAL SUBSYSTEM	4/16	4/16	4/12	4/12	4/12	1/2	4/8	3/9	2/10	5/10	3/12	1	119
RECEIVER SUBSYSTEM	5/20	5/20	5/15	4/12	5/15	5/10	5/10	4/12	4/20	3/6	4/16	1	156

Figure 2. Evaluation and Selection Criteria Plan Scores for Both Concepts

3.0 CONFIGURATION SELECTION

Having selected a concept for LAWS we went on to define the system requirements in detail, develop the system functional block diagram and produce preliminary design configurations for the major subsystems and for the integrated instrument.

3.1 Baseline Specification

The functional block diagram (see Figure 3) identifies the major subsystems, i.e. the laser transmitter, the optics and the receiver, and the supporting subsystems (identified with an "S"). The diagram is used to identify the interfaces and facilitate trades between the subsystems.

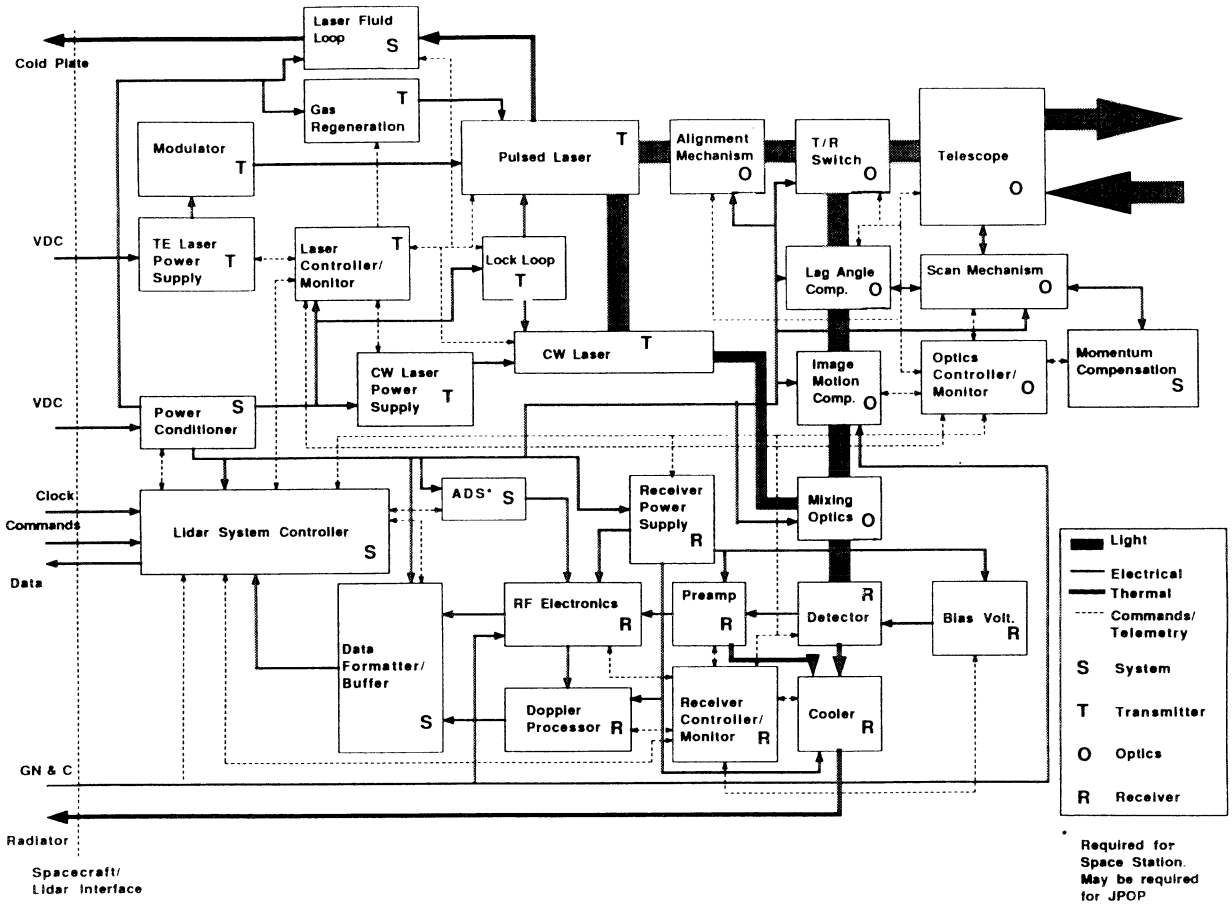

Figure 3. LAWS System Functional Block Diagram

After a detailed system analysis we arrived at the following specification from which to proceed with the configuration definition:

Laser Energy per Pulse	10 Joules;
Laser Pulse Repetition Rate	Asynchronous, 20 Hz max.;
Pulse Length	3 μsec;
Telescope Aperture	1.5 m;
Conical Scan Angle	45°;
Telescope Rotation Rate	12 rpm.

The energy per pulse, telescope aperture, pulse length and nadir angle influence the accuracy of the line-of-sight velocity; the nadir angle, laser repetition rate and telescope rotation rate determine the shot pattern laid down on the ground and hence influence the fidelity of the horizontal inversion. The choice of a laser capable of firing asynchronously (up to some maximum rate) is key to providing a versatile system which can use simple (e.g. selectively inhibiting laser firing over the poles on some orbits) or sophisticated (e.g. laser firing based on the telescope azimuth angle) shot management algorithms to make best use of the laser shots available. Such a capability also allows power-saving strategies to be implemented with minimum impact on science return.

From this baseline specification and accommodation constraints imposed by the platform, detailed configurations for the three major subsystems, the laser, the optics and the receiver, were developed.

3.2 Laser Subsystem

The laser subsystem consists of all the components required for the generation and frequency control of two CO_2 laser beams, the transmitter and local oscillator. The selected transmitter architecture is the external injection of a transversely excited, transverse flow oscillator incorporating an unstable resonator cavity. The external injection selection is based on the heritage of this approach for long-range wind sensing, and in its high-power potential, since the high gain possible with this design allows an unstable mode to be generated. This results in efficient use of the gain medium.

The transmitter laser generates a continuous train of single frequency pulses (10 J, 3 μsec) at an average rate of 10 Hz (20 Hz peak), that is delivered to the optical subsystem for transmission to earth. The frequency of the transmitter laser is controlled by injecting it with a sample of a 5-Watt, highly-stable, continuous-wave (cw) laser beam. Another sample is delivered to the receiver subsystem to function as the local oscillator beam. A functional block diagram of the laser subsystem is shown in Figure 4. It consists of four major modules: the transmitter gain, optical, control and diagnostics, and auxiliary modules, respectively.

The *transmitter gain module* conditions and excites the laser gas and is attached to the instrument platform using vibration isolation mounts to protect the instrument from vibrational perturbations. Self sustained discharge excitation of the gas was chosen for reasons of simplicity and efficiency, and was supported by experiments at Spectra Technology conducted under a program jointly funded by the NASA Marshall Space Flight Center and the Air Force Geophysics Laboratory. This investigation provided

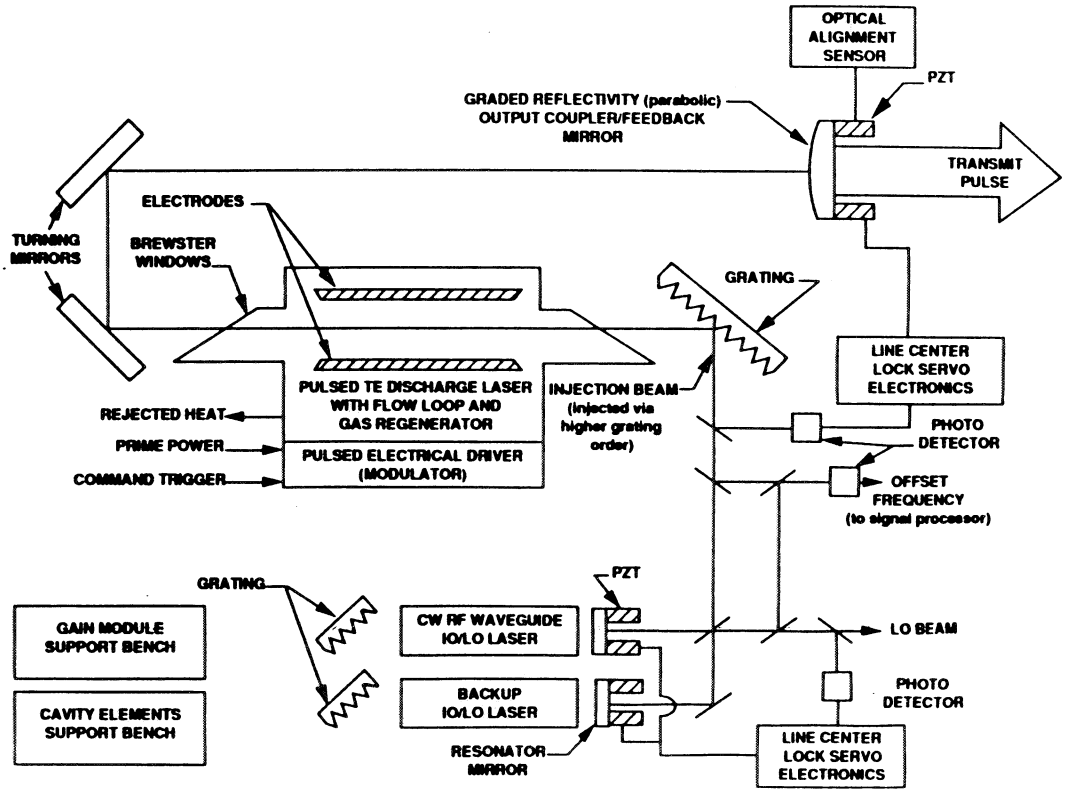

Figure 4. Functional Block Diagram of the Laser Subsystem

measurements of the laser gain coefficient and collisional relaxation rates for the $^{12}C^{18}O_2$ rare isotope gas mixtures, which were used in our laser modeling and scaling studies, and also produced efficiencies of the self-sustained and e-beam sustained discharge approaches. Intrinsic efficiencies exceeding those measured using the e-beam sustained approach were observed.

Pulse profile predictions using the measured kinetic rates in conjunction with Spectra Technology laser kinetic codes are in excellent agreement. The parameters of

the transmitter gain section were established using these codes, and used as the basis for the configuration development and size-weight-efficiency estimations. The baseline configuration uses a gas mix of 3 parts He, 2 parts N_2 and 1 part CO_2 (3/2/1), the same as was used in the MSFC/AFGL Study. Experiments were also undertaken to investigate gas degradation under self-sustained (as opposed to e-beam sustained) conditions which confirmed that gas regeneration can be accommodated with a modest catalyst bed.

The transmitter gain module configuration is shown in Figure 5. The gain module shell is made out of graphite-epoxy material which makes for a lightweight structure. The pulsed power system, the flow loop which circulates the gas through the laser cavity, the catalytic converter, heat exchanger and acoustic dampers are all integrated into the laser gain module shell, ensuring a very compact structure.

The *optical module* is the host for all the optical components including the laser resonator and beam sampling and control optics and is vibrationally decoupled from both the gain module and the instrument platform such that it experiences a quiescent vibrational environment. The integrated laser subsystem is depicted in Figure 6 and shows the graphite-epoxy truss structure that supports the optical benches at either end of the transmitter gain module. The unstable resonator configuration selected uses a graded reflectivity mirror for the feedback/output coupler because of superior mode discrimination and the excellent output beam quality characteristics of this arrangement, e.g. the >80% conversion of the transmitted energy into the central lobe in the far field. A fixed frequency waveguide laser was chosen as the injection/local oscillator for reasons of simplicity and robustness. Our current design includes a second unit for redundancy.

The *control and diagnostics module* accomplishes sequencing of laser operation and conducts system health checks. It is basically a central processor that accepts commands from the LAWS system controller and in turn provides the laser fire control signal, samples status and health sensors and relays the information to the system controller. It also relays pulse frequency information to the Doppler signal processor (in the receiver), implements the laser alignment and frequency control logic and provides control signals.

The *auxiliary module* provides for all ground support functions during ground testing through on-orbit operation. Included in this module are the thermal control system, gas supply, protective cover and calibration equipment.

The laser subsystem weighs 141 kg and operates at a baseline efficiency of 6%, with a goal of 7.5%.

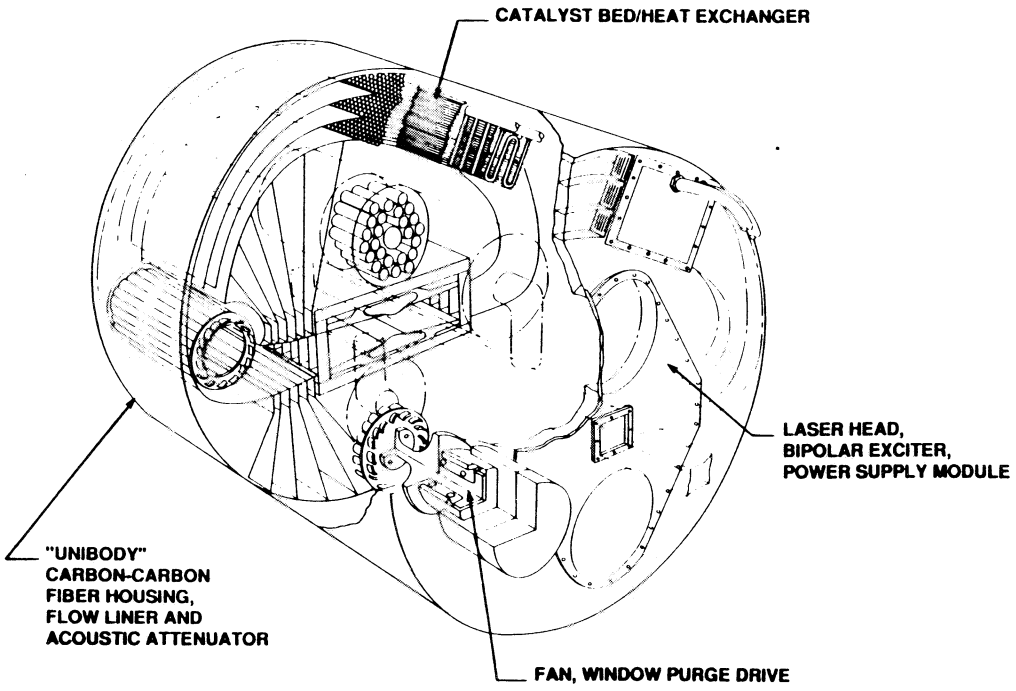

Figure 5. Transmitter Gain Module Configuration

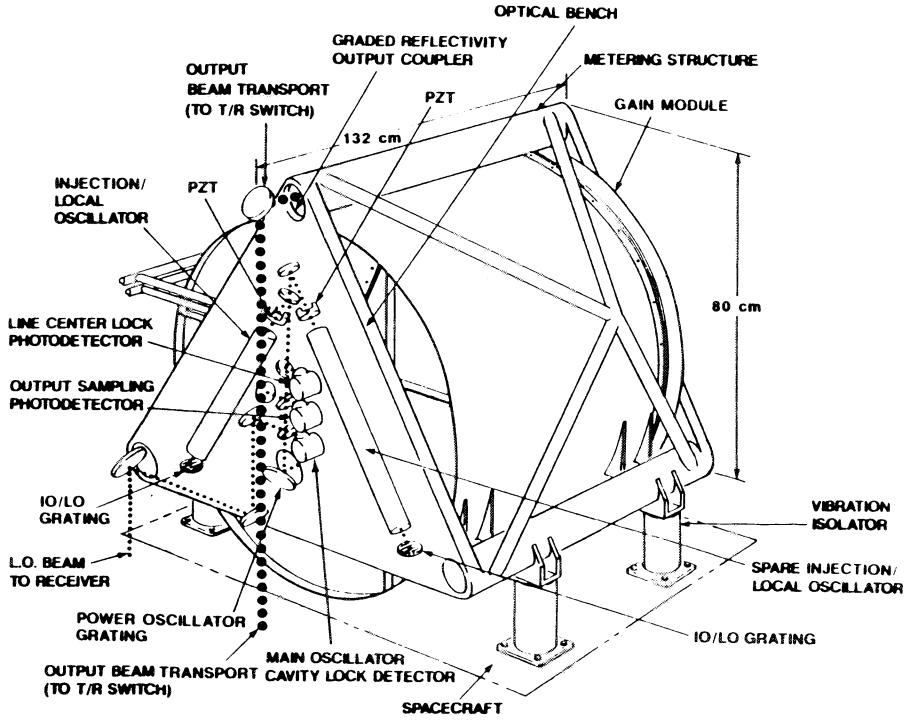

Figure 6. Integrated Laser Subsystem

The issues associated with the laser subsystem which have been identified during the Phase I Study fall into three categories. They are 1) those issues associated with using $^{12}C^{18}O_2$ in the discharge, 2) issues associated with component reliability, and 3) the verification of LAWS-scale performance and lifetime. $^{12}C^{18}O_2$ issues have been largely resolved by the MSFC/AFGL Study mentioned previously; catalysts for $^{12}C^{18}O_2$ continue to be investigated by NASA LaRC and others. Component reliability studies are being addressed by a number of DoD and internally funded programs, and the NASA Laser Breadboard Program will address LAWS-scale verification and lifetime.

3.3 Optical Subsystem

The block diagram of the optical subsystem is shown in Figure 7. It consists principally of the following functional elements:

- the conically scanning telescope with its mechanical support structure and scan bearing assembly;
- image motion compensation (IMC) and lag angle compensation (LAC) optics;
- the mixing optics and,
- an alignment and pointing control subsystem.

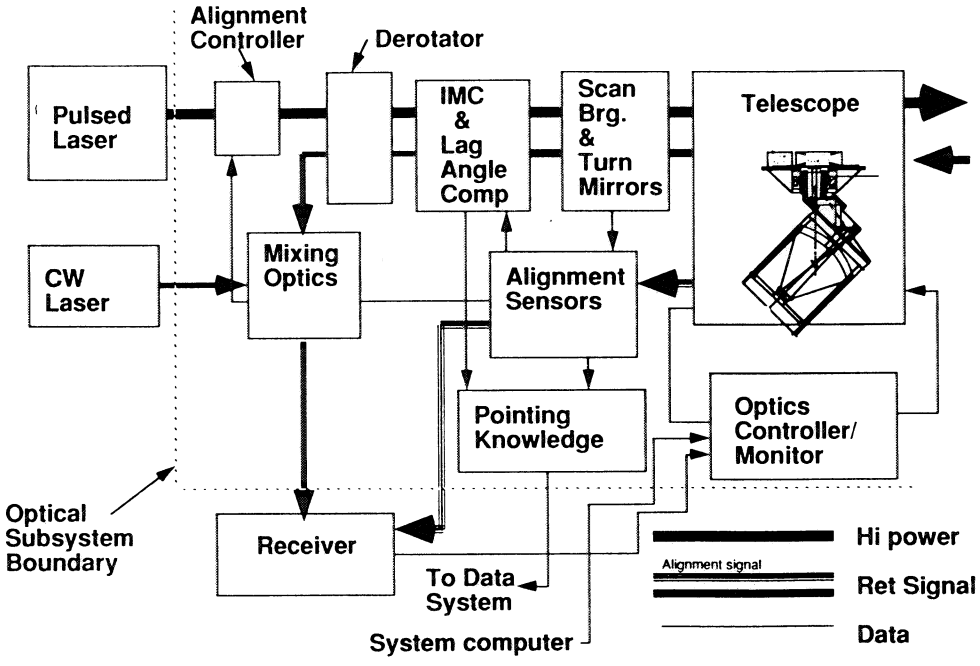

Figure 7. Optical Subsystem Functional Block Diagram

One of the key, early studies for space-based wind sensors was the Windsat study which considered flying a CO_2 Doppler lidar on board the Space Shuttle. Hughes Danbury Optical Systems, formerly Perkin-Elmer, was responsible for the optical subsystem design. During the LAWS Phase I Study Hughes Danbury revisited the optical subsystem design to consider the new requirements imposed by the JPOP platform (principally weight) and also to address certain shortcomings inherent in the Windsat optics. These shortcomings included the presence of focal points in the optical train which would lead to air breakdown when the laser beam passed through them (making it impossible to test the integrated system in air) and excessive optical feedback to the laser, which could cause it to become unstable. Hughes Danbury responded to these challenges by developing a new optical design which is less complex than the original Windsat design and offers an improved optical efficiency and lower weight.

The new design uses a two-mirror, confocal parabola telescope (shown on the left-side of Figure 8). In the earlier Windsat studies, the optical design was a three-mirror system with an accessible exit pupil. The purpose of the accessible pupil was to incorporate a rotating polygon (or equivalent) to compensate for the lag angle. The rotating polygon did not allow asynchronous laser operation, however, and so we eliminated it from the design. The lag angle is now accommodated by a fixed offset. Using this offset to compensate for the lag angle also allows us to remove the transmit/receive switch from the design since the transmit and receive optical paths are physically separated. The Image Motion Compensation (IMC) mirror, based on space-qualified hardware, removes any random lag angle variations during pulse reception, as well as other small predictable changes such as those caused by altitude variations.

A comparison of the Windsat and confocal parabola optical designs is shown in Table 1. For every criterion the confocal design is superior.

The Windsat telescope mechanical design was also improved to provide an opto-mechanical design that meets the weight requirements with margin. The mechanical configuration (shown on the right-side of Figure 8), is the result of an extended trade study directed toward the minimum weight and cost LAWS configuration.

Another important element of the optical subsystem is the method by which the laser, telescope and receiver axes are maintained in coalignment in the dynamic and static environments of the conically scanning telescope and the varying thermal environment of the orbiting platform. Such alignments are a challenge since they must be maintained to sub-arcsecond stability. We have been able, however, to exploit some recent Hughes Danbury developments in large laser beam expanders to support the LAWS

design study and baseline an alignment and controls subsystem which will assure robust optical alignment and image motion control.

Criteria	Windsat	Confocal Parabola
Central Obscuration	16%	<1%
Beam Quality	0.05 λ rms	0.026 λ rms
Number of Optical Elements	19	14
Number of Mechanisms	3	2
Internal Focus (Restricts Testing)	Yes	No
Lag Angle Compensation	With Mechanism	Precomputed and Fixed
Optical Feedback	High	<<0.01%

Table 1. Comparison of Optical Designs

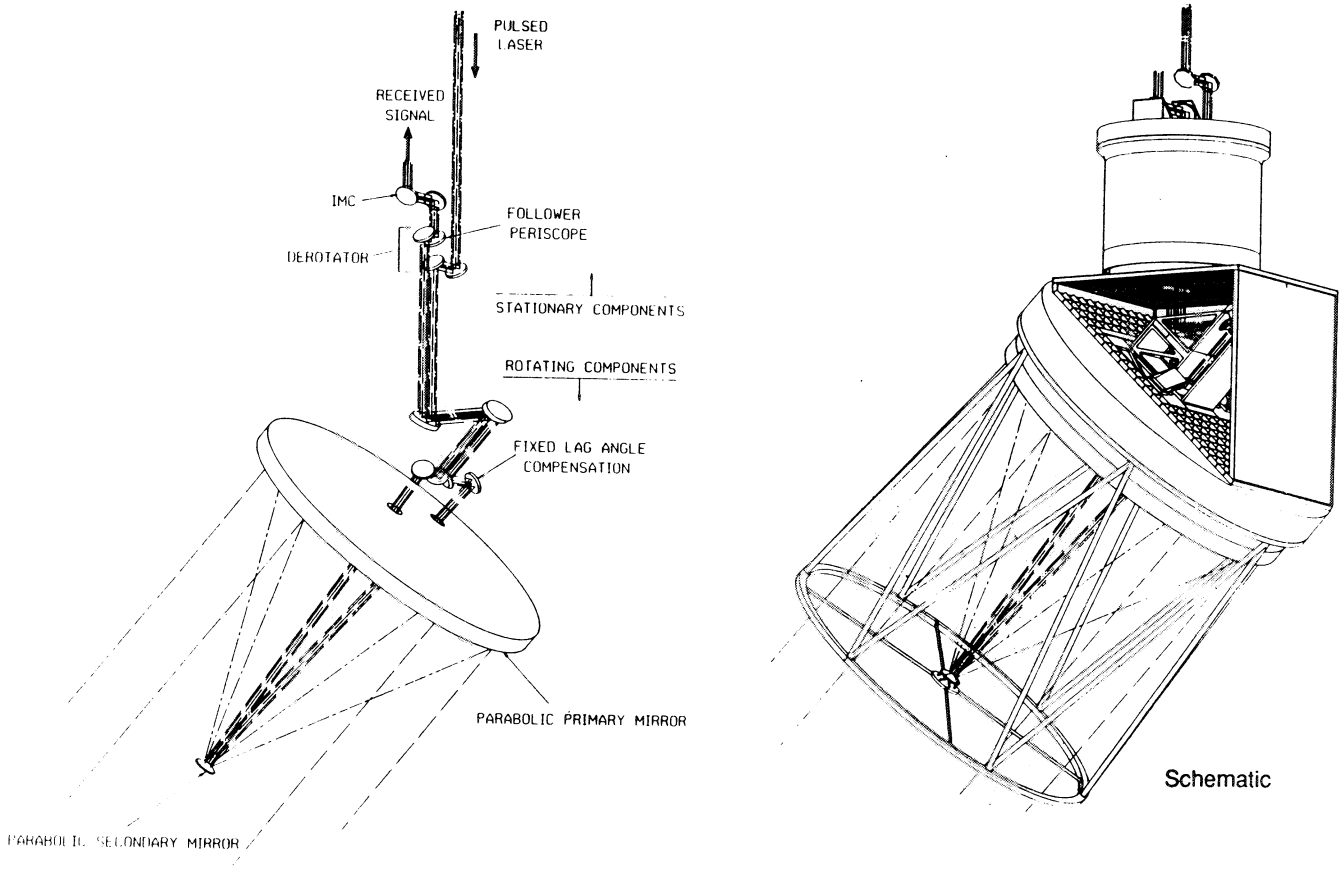

Figure 8. Confocal Parabola: Optical and Mechanical Schematic

The issues associated with the optical subsystem which have been identified during the Phase I Study are 1) the tight pointing requirement over the round trip time, 2) the establishment and maintenance of the transmit/receive axis alignment and 3) weight. Pointing and alignment issues have been addressed by previously funded programs and continue to be the focus of ongoing work at Hughes Danbury.

In order to reduce the weight of the optical subsystem extensive use will be made of lightweight materials (e.g. Beryllium, Silicon Carbide) and composites.

3.4 Receiver Subsystem

The functional block diagram of the receiver subsystem is shown in Figure 9. The receiver subsystem is made up of the Mercury-Cadmium-Telluride (MCT) detector, the detector pre-amplifiers, the cooler and receiver electronics. The electronics consists of the intermediate frequency (IF), amplifier, the complex demodulator, the signal processing, the subsystem controller/monitor, and the subsystem power supply.

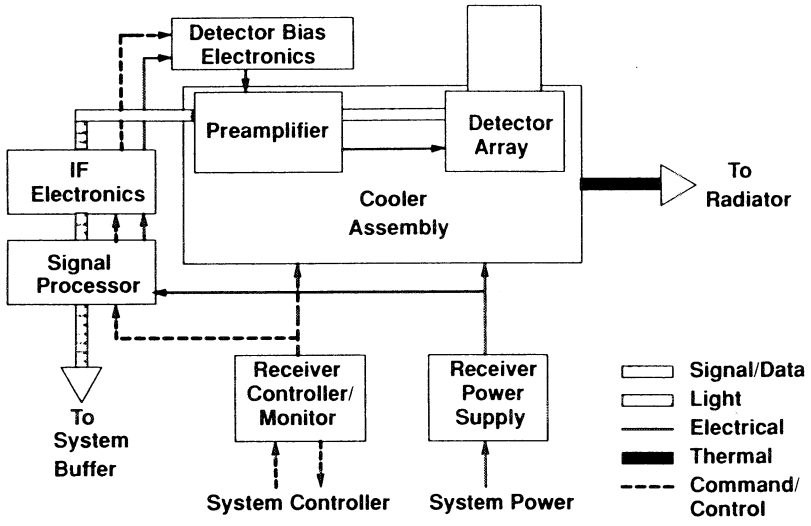

Figure 9. Receiver Subsystem Functional Block Diagram

The baseline MCT detector consists of a circularly symmetric array with a central element of optimum size, surrounded by four alignment elements (see Figure 10). The array is used to provide an end-to-end system measurement of the alignment of the return beam on the detector using strong signal returns, and to measure the phase and intensity map of the signal at the focal plane for use in wavefront correction or

optimization of coherent signal combination. This provides the means to continuously monitor LAWS total system alignment and thereby assure optimum performance.

The array design also provides some degree of improved performance over an optimally sized single detector under perfectly aligned conditions (the four surrounding elements receive the energy contained in the first bright ring of the Airy pattern). However, for small misalignments of the return beam the array provides significantly improved performance over a single detector and allows a reduction in the optical alignment tolerance.

The central detector element of the array has the optimum size for a single detector. Heterodyne mixing efficiency analysis has shown that this optimum size is 74% of the Airy disk diameter when using a flood illuminated local oscillator (LO) and diffraction limited optics.

The baseline preamplifier for the LAWS receiver is a GaAs Field Effect Transistor (FET) cooled to 120 K. Cooling reduces the noise figure to around 0.5 dB while still maintaining a gain of about 10 dB. Each of the detector elements has a separate preamplifier which again provides redundancy in the design.

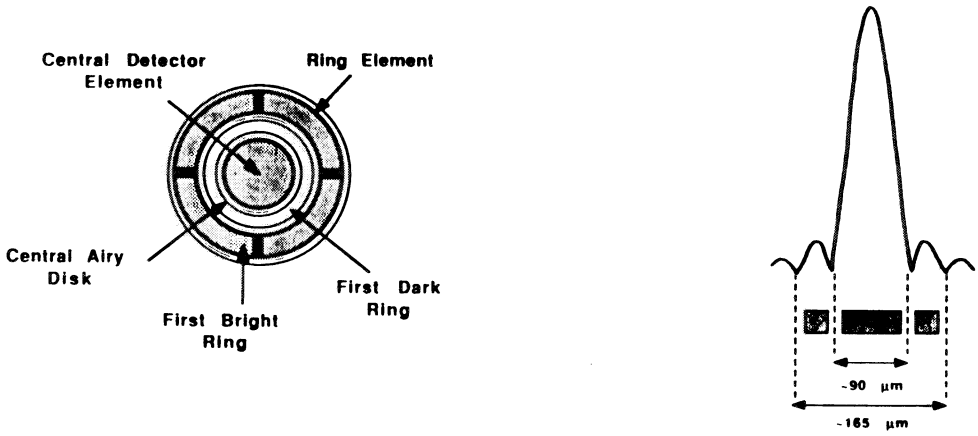

Figure 10. Detector Geometry

The cooler approach is based on the split Stirling cooler presently being developed for a variety of long-life space missions including the Upper Atmospheric Research Satellite (UARS) ISAMS instrument. The combination of fairly large heat loads

(around 5 Watts total), the low temperatures required (80 K for the detector and 120 K for the pre-amplifiers), mission lifetime requirements, and technology maturity results in the split Stirling cooler as the primary choice. The cooler configuration consists of a pair of opposed Stirling engines to minimize vibration.

The IF amplification stage which includes removal of the satellite-induced Doppler shift and coherent demodulation, is shown in Figure 11. The coherent homodyne, or "COHO", approach was chosen to reduce the A/D conversion rate as well as to improve the Doppler estimator accuracy. A logarithm channel is included for measuring strong signals from clouds or the ground. Following the IF electronics is an analogue-to-digital converter and the signal processing electronics. Each of the five channels of the detector array will have separate IF electronics and signal processing hardware. Again, this provides maximum redundancy, as well as robustness, by providing extra processing power which may be reconfigured on-orbit. The remainder of the receiver electronics includes a subsystem controller/monitor to provide input/output to the LAWS system controller and a power convertor for conversion of the spacecraft power to that required by the receiver subsystem.

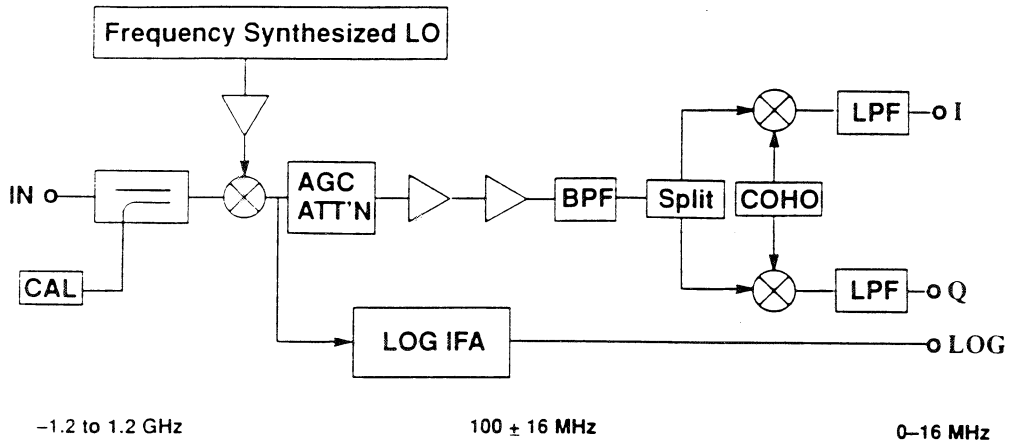

Figure 11. IF Electronics Schematic

The technical issues associated with the receiver subsystem which have been identified during the Phase I Study are 1) improving the performance of MCT detectors, 2) the cooler requirements for the detector and preamplifiers, and 3) the Doppler estimator performance. MCT detector improvements are the subject of a number of DoD programs as well as in-house efforts at GE. Split Sterling coolers with the capability required for LAWS are being developed by NASA, Ball Aerospace, and British Aerospace

for application on the EOS program. Finally, improved Doppler estimators are under development by Lassen Research and members of the LAWS Science Team.

3.5 Integrated System Description

LAWS is a candidate payload for the Japanese Polar Orbiting Platform (JPOP) and U.S. Space Station. At the time of the LAWS Phase I Study the design of JPOP was in a very early stage and details as to mechanical, thermal, and electrical instrument accommodation requirements were not available. To develop concepts for mounting LAWS to JPOP we therefore needed a surrogate platform which was representative of what could be expected as the JPOP design matured. Since NASA, Europe and Japan are all involved in the Earth observing system (EOS) program, we selected a platform concept based upon EOS-A, for which GE is the developer and systems integrator, to study our approach to instrument accommodation. EOS-A has been selected for launch on a Titan-IV which has an envelope of 15 ft (4.6 m) identical to the full-sized Japanese H-II launch vehicle envelope.

Two views of LAWS accommodated on the EOS-type platform are shown in Figure 12. The instrument has been divided into two parts for ease of accommodation. Mounted to the front of the platform is the sensor module which consists of the telescope, the laser and the receiver assemblies. A support module is mounted on the earth facing panel of the end bay of the platform. The support module takes up two of the payload mounting plate locations on the end bay. One plate supports the laser fluid circulation system, the system controller, power conditioner and momentum wheel. Heat from these components is dissipated through a platform-supplied cold plate. Alongside this plate is the laser heat exchanger and cold plate assembly, which has been sized to dissipate an average of 2 kW.

The thermal subsystem also comprises two parts. The laser heat rejection subsystem uses a cold plate to dump heat from the laser on to the platform thermal bus. As stated above the laser heat rejection subsystem is sized to reject 2 kW, which allows an average laser repetition rate of about 13 Hz. The design allows the laser burst mode of 20 Hz to be sustained for 1-2 minutes.

The second part of the thermal subsystem is a local radiator attached to the sensor module which rejects heat from the receiver cooler assembly and other electronics boxes. The radiator faces the anti-sun side and has an area of 15 sq. ft.

Our analysis of the electrical power required from the platform to operate LAWS has assumed a 6% efficient laser operating at the nominal average rate of 13 Hz during a

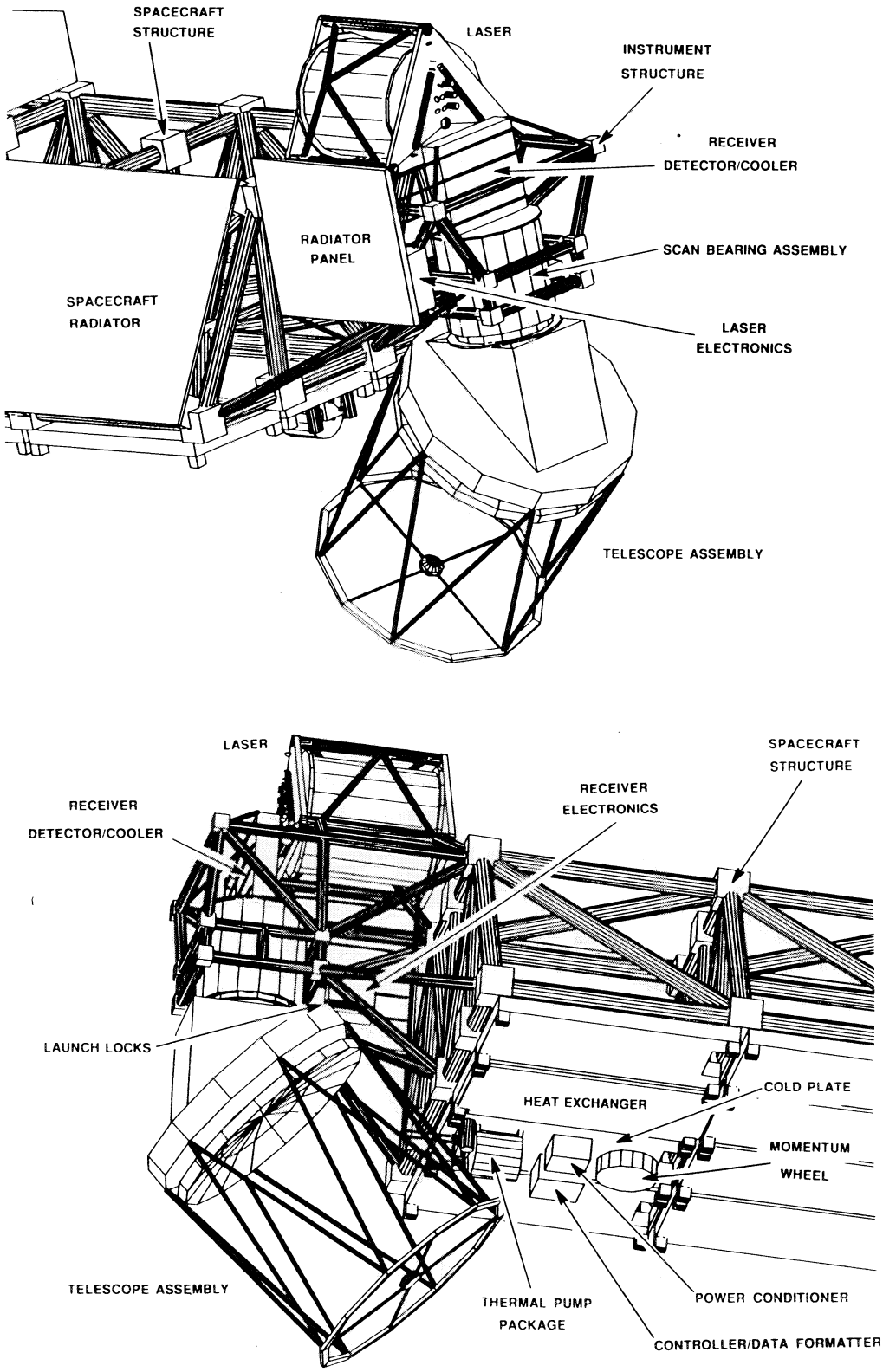

Figure 12. LAWS Integrated System Configuration

single scan. This represents a 20 Hz laser operating according to a simple shot management algorithm based on 1/cos of the azimuthal angle (note that other shot-firing algorithms are possible with an asynchronous laser). We also assumed a 90% duty factor during an orbit since oversampling at high latitudes allows for a reduced repetition rate. The 90% number is conservative; the actual opportunities for shot suppression at high latitudes are about 22% for an orbit altitude of 824 km.

Under these assumptions the average power requirement is 2735 W (2935 W with a 7% reserve). In practice over the lifetime of the instrument we will have an average rate of 10 Hz, which gives a power consumption of about 2470 W (2840 W with 15% reserve). For the same 1/cos algorithm and a 10 Hz maximum repetition rate laser, the power requirement becomes 1835 W (2110 W with 15% reserve). If the design goal of 7.5% laser efficiency is achieved, then either a higher average pulse rate or a lower average power system would become available.

If the platform orbit altitude were to be lowered to 705 km the power requirements could be reduced further to 1975 W (10 Hz, 1/cos algorithm) for the same performance and coverage as at 824 km (note, to obtain same coverage the scan angle is increased to 49°).

A summary breakdown of the LAWS system configuration parameters, including all the major subsystems, for the JPOP platform is shown in Table 2.

Component Description	Weight (kg)	Average Power (W)	Standby Power (W)
Laser Subsystem	141	1889	30
Optical Subsystem	334	212	81
Receiver Subsystem	40	280	200
Support Subsystems	43	153	23
Thermal Subsystem	55	200	200
Mechanical Structure	67	0	0
Total	680	2734	534
Reserve	102	200	80
Total + Reserve	782	2934 *	614

** 2110 W for 10 Hz 1/cos operational mode (824 km)*

Table 2. LAWS System Configuration Parameters

LAWS has stringent alignment tolerances and requires a very stiff support structure with a high degree of thermal stability. For this reason the sensor module is supported by a graphite-epoxy truss structure with titanium fittings. The design has

been based on GE's UARS structure technology which is also being used on the U.S. Polar Platform designs being developed by GE.

Figure 13 shows a side view of the platform in its launch configuration inside the Titan IV shroud. The platform laser heat rejection radiator runs the whole length of the platform from the instrument module to the propulsion module.

Figure 14 shows the LAWS instrument reconfigured as an attached payload for the manned Space Station. The telescope, laser and receiver are mounted on the same side of a deck carrier and the telescope is raised about 6" to accommodate the input and output beams. The assumption has been made that the instrument heat rejection would be handled by a Space Station thermal control subsystem. If the instrument had to carry its own radiator it would require a radiator area of about 180 sq. ft. An analysis has shown that there is sufficient room for two 6 ft. x 15 ft. radiators which could be deployed and steered to offer the most favorable thermal rejection.

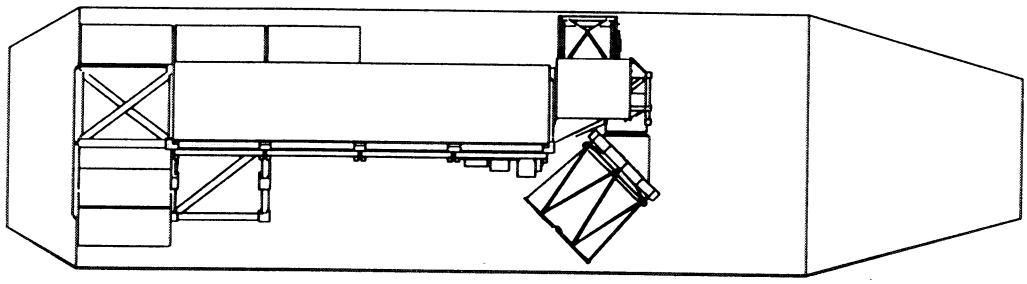

Figure 13. LAWS Platform Inside the Titan Shroud

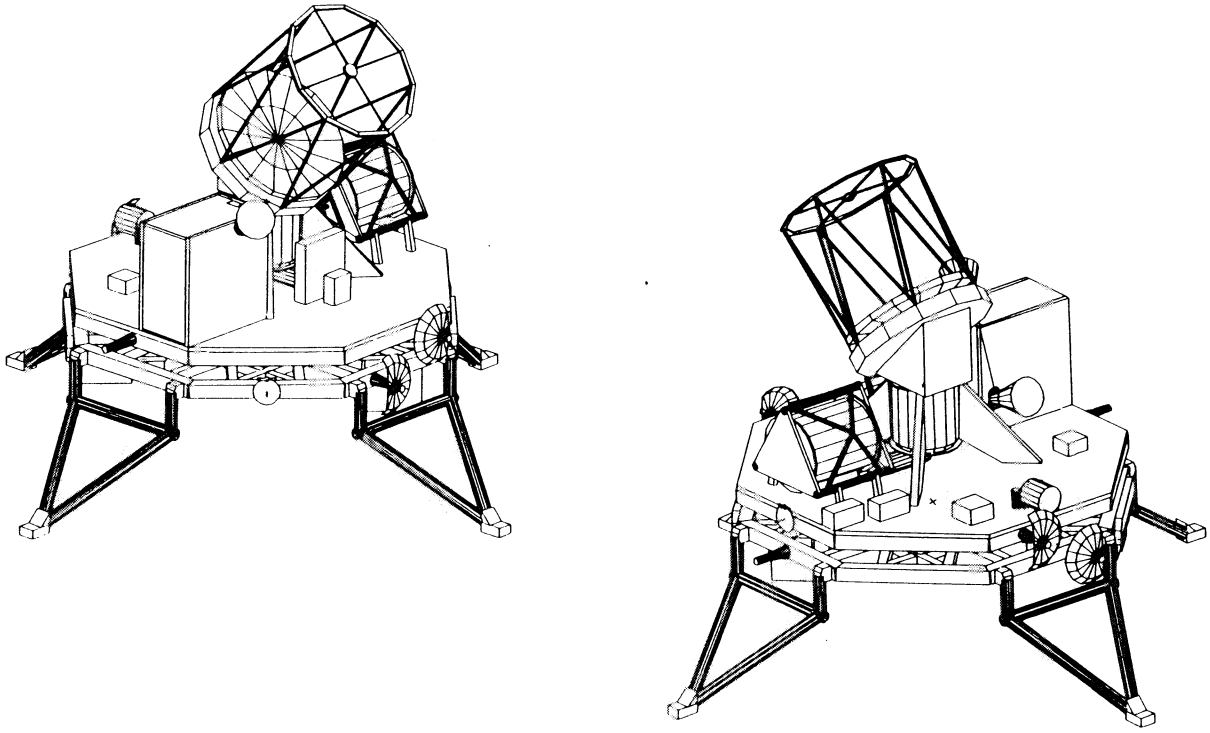

Figure 14. LAWS Configured as an Attached Payload on Space Station

4.0 LAWS SYSTEM PERFORMANCE

The configuration discussed above meets the performance requirements for LAWS. Analysis results are given below in terms of coverage, signal-to-noise ratio (SNR), line-of-sight (LOS) velocity error and horizontal inversion accuracy.

Given a circular polar orbit, an 824 km altitude and a 45 degree scan angle, the percent coverage has been calculated for both a 12 and 24 hour period. These percent coverage plots, Figure 15, show that in 24 hours there is 100% coverage except in the latitudes between about 5 and 35 degrees, where the coverage falls to a minimum of 75%, due to ground track overlap at these latitudes. Note that this coverage analysis is a measure of shot placement and does not address obscuration by clouds.

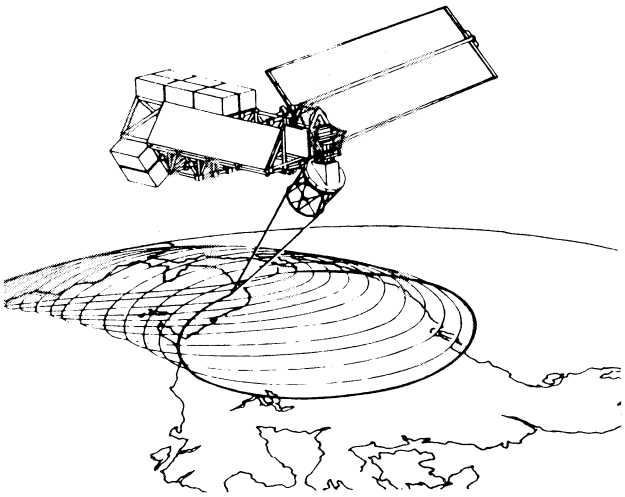

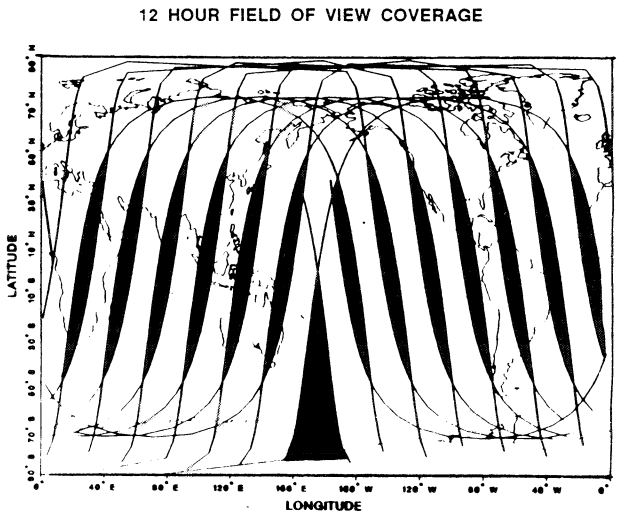

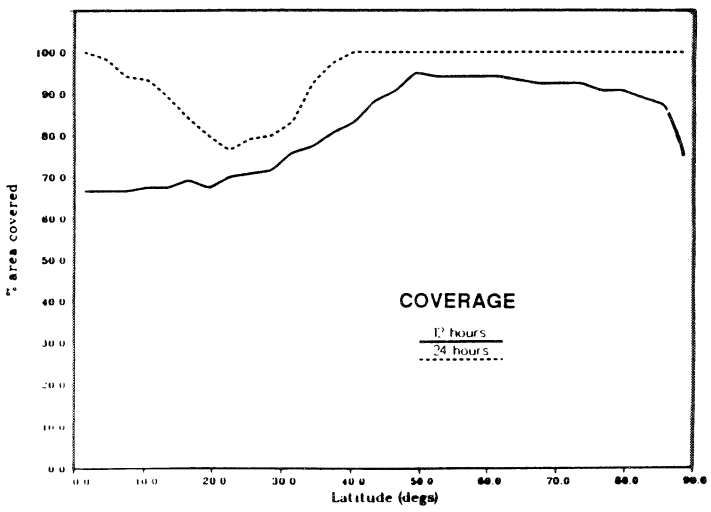

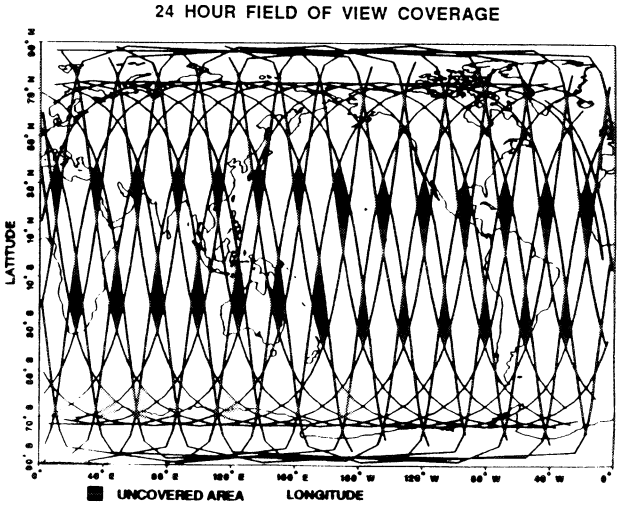

Figure 15. Coverage for 824 km Orbit

In order to determine the LOS SNR a baseline backscatter profile must be defined. The left side of Figure 16 shows the median value of the baseline backscatter distribution provided by NASA for use in the Phase I Study. The two curves represent the cases with and without high altitude cirrus cloud enhancement. These median backscatter values, along with the subsystem parameters can then be used in the lidar equation to estimate the LAWS narrow band SNR which is presented on the right side of Figure 16. The minimum SNR for the upper troposphere, without cirrus enhancement, is -6.5 dB which is sufficient to provide the required 5 m/s LOS velocity over a 100 x 100 x 2 km volume (as described below).

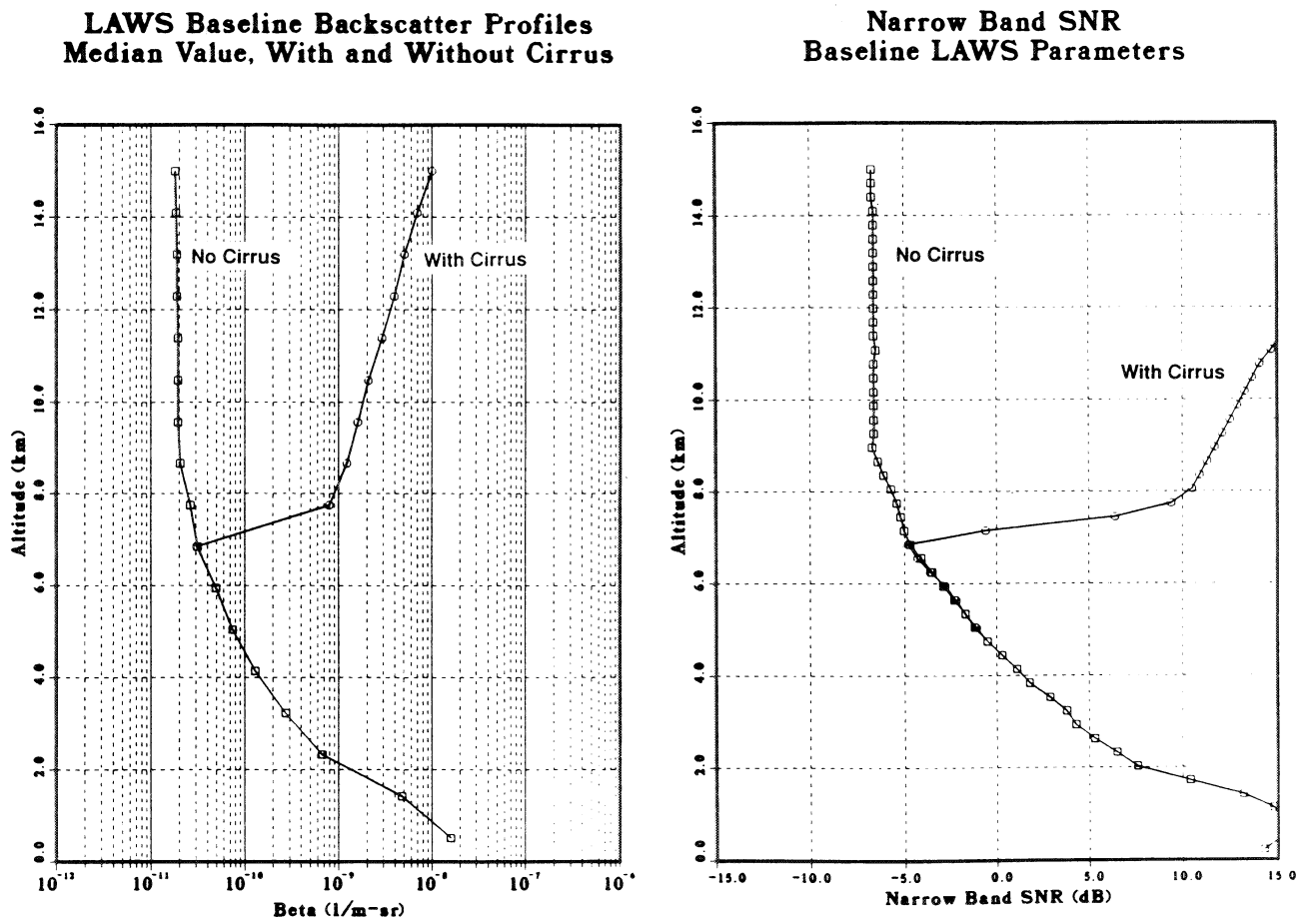

Figure 16. Baseline LAWS Performance

If we include the statistics of the backscatter distribution we can plot the probabilities of achieving certain values of the SNR. This is shown in Figure 17 for SNR values of -5, 0, and 5 dB as a function of altitude, showing both the background and cirrus enhanced beta profiles. This analysis provides an indication of the range of instrument performance that can be expected due to variations in atmospheric backscatter.

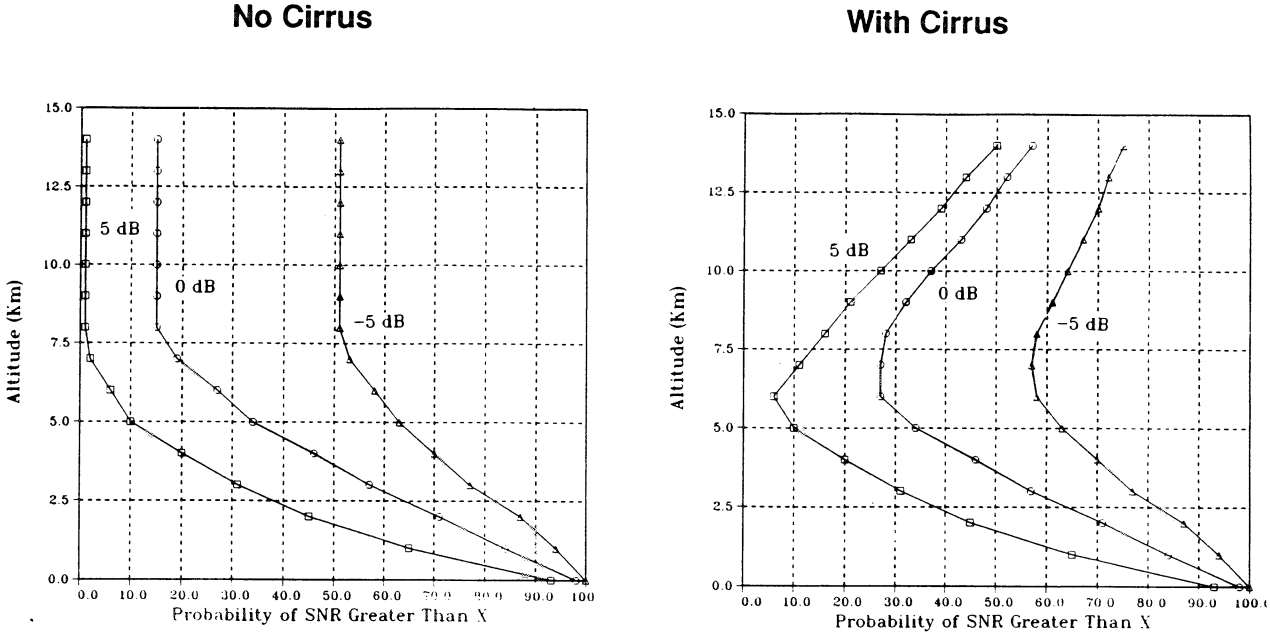

Figure 17. Probability of Achieving SNR Values of -5, 0 and 5 dB.

A large variety of Doppler processing algorithms are available for the estimation of LOS velocity. Figure 18 is a plot comparing the Cramer-Rao lower bound estimate (theoretical limit) with an Adaptive Poly-Pulse Pair (APPP) estimator (developed by GE and Lassen Research (R.Lee)). With the SNR profile (no-cirrus case) shown in Figure 16, the APPP estimate (labeled Lee in the figure) gives a 7 m/s median error in the upper troposphere using a 100 x 100 x 1 km volume. This error is reduced to less than 5 m/s if the estimate is made using a 2 km vertical resolution above 6 km. In the presence of cirrus the LOS velocity estimate is about 0.4 m/s.

Finally, the estimates of LOS velocity can be input to a least squares horizontal inversion algorithm to estimate the horizontal velocity vector. This has been performed using the median LOS velocity error estimates in Figure 18 and the results presented in Figure 19. Two specific realizations show the horizontal inversion performance for a

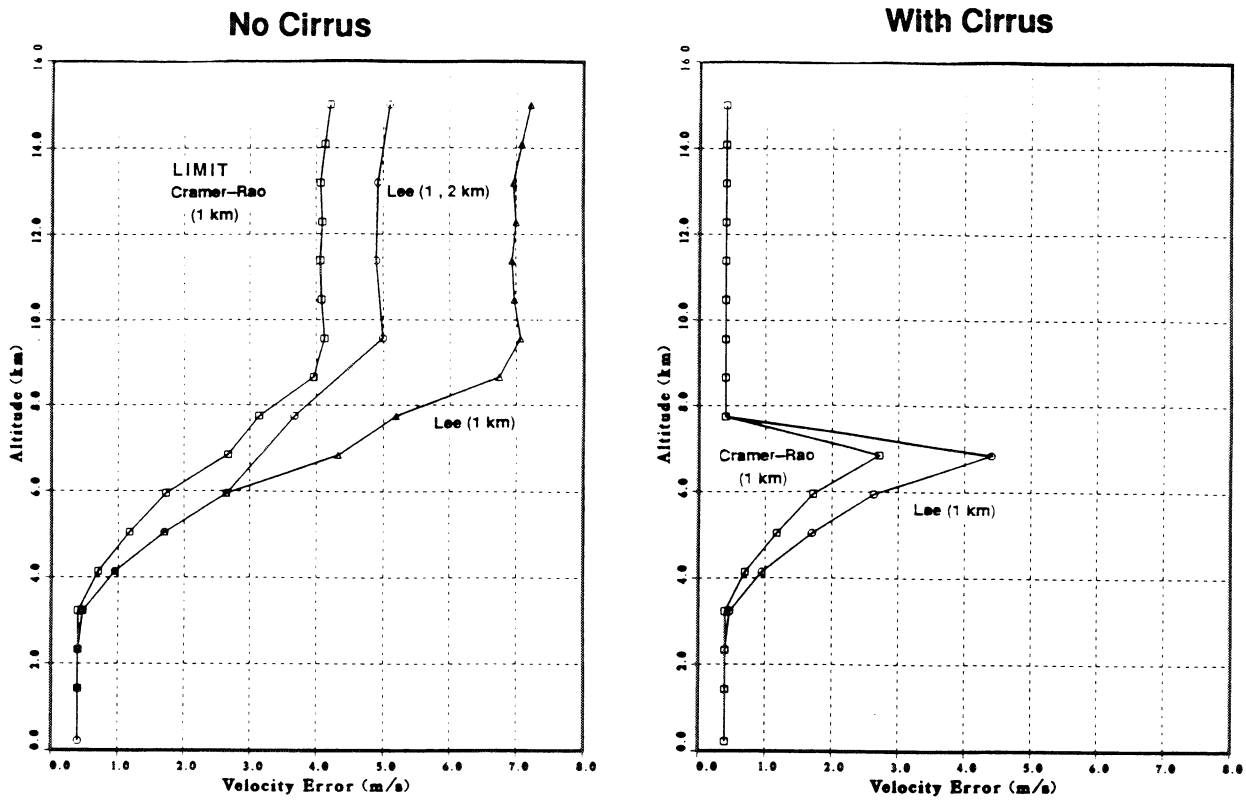

Figure 18. Line-of-Sight Velocity Error Estimates

4.5 and 12 km altitude. At the lower altitude the 100 x 100 x 1 km resolution was used, while a 2 km vertical resolution was used at the higher altitude. The cell numbers in the figure represent the nine, cross-track, 100 by 100 km cells within one-half of the conical scan with cell 1 being the closest to the suborbital track and cell 9 being at the extreme of the scan. In both cases the uncertainties in cells 1 and 9 are large due to the poor two-dimensional sampling of the horizontal vector (the LOS vectors are not sufficiently well separated in angle); however, elsewhere the velocity uncertainty and wind direction are generally within the system requirements of 1 m/s at low altitudes and 5 m/s in the upper troposphere. With cirrus present the SNR is sufficient to provide 1 m/s horizontal wind estimates in the upper troposphere.

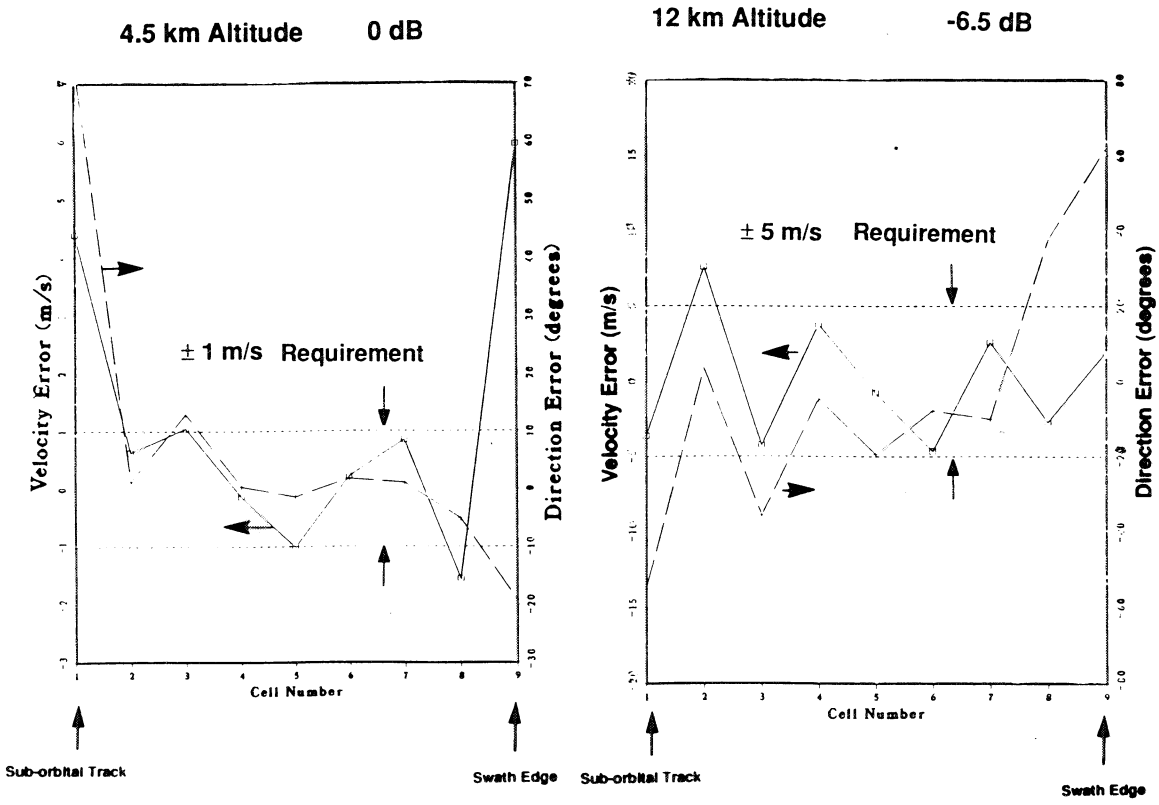

Figure 19. Horizontal Inversion Realizations

The preceding performance analysis shows that the science requirements are met with the baseline LAWS system configuration. Further improvements in signal processing and more advanced horizontal inversion techniques will provide additional margin in meeting the horizontal wind velocity requirements.